The Research of Medical Science Review
ISSN: 3007-1208 & 3007-1216 Volume 3, Issue 8, 2025

INTEGRATIVE IMMUNOINFORMATICS DESIGN OF A MULTI-EPITOPE PEPTIDE VACCINE TARGETING CONSERVED FLAGELLIN A PROTEIN OF MULTIDRUG-RESISTANT PSEUDOMONAS AERUGINOSA

Haris Munir[1], Hamna Tariq[1], Muhammad Saleem[1], Ali Noman[2], Kainat Ramzan[*3], Amina Islam[4], Ibtsam Bilal[3], Aamer Hassan[1], Moeen Zulfiqar[1], Ali Moazzam Qadri[1], Ali Haider Ali[3], Syed Arslan Haider[1], Isfa Sarfraz[1]

[1]*Department of Molecular Biology, University of Okara, Punjab, Pakistan*
[2]*Department of Zoology, University of Okara, Punjab, Pakistan*
[*3]*Department of Biochemistry, University of Okara, Punjab, Pakistan*
[4]*Department of Microbiology and Molecular Genetics, University of Okara, Punjab, Pakistan*

[*3]kainat.ramzan@uo.edu.pk

DOI: https://doi.org/10.5281/zenodo.16785393

Keywords
Antigenicity, Codon optimization, Epitope, Flagellin A, Immunoinformatics, P. aeruginosa, Vaccine design

Article History
Received on 08 May 2025
Accepted on 14 July 2025
Published on 09 August 2025

Corresponding Author: *
Kainat Ramzan

Abstract

Pseudomonas aeruginosa *is a multidrug-resistant pathogen that poses a serious threat to immunocompromised individuals, necessitating novel vaccine strategies. This study employed an integrative immunoinformatics and structural bioinformatics approach to design a multi-epitope peptide vaccine targeting the conserved Flagellin A protein of* P. aeruginosa. *B-cell, cytotoxic T lymphocyte (CTL), and helper T lymphocyte (HTL) epitopes were identified and screened based on antigenicity, non-allergenicity, and human non-homology. The selected epitopes were assembled into eight vaccine constructs using appropriate linkers and adjuvants, and modeled using AlphaFold v3. Among them, construct 7 emerged as the most promising candidate, exhibiting superior structural stability (ERRAT score: 98.27; >90% residues in favored Ramachandran regions) and optimal physicochemical properties, including a low instability index and high solubility. Molecular docking demonstrated strong binding affinities of the epitopes with MHC class I (HLA-A11:01), MHC class II (HLA-DQB1*03:01), and innate immune receptors TLR4 and TLR5, with binding energies as low as −189.76 kcal/mol. Immune simulations predicted strong IgG and IgM responses, T-cell activation, and cytokine release, indicating a balanced humoral and cellular immune response. Codon optimization (CAI: 1.0; GC content: 53.03%) and in silico cloning into the pET28a (+) vector confirmed high expression potential in* E. coli *K12, supported by favorable mRNA structure and ribosomal docking. Overall, construct 7 represents a stable, immunogenic, and expressible vaccine candidate, offering a promising avenue for future experimental validation against* P. aeruginosa *infections.*

INTRODUCTION

Pseudomonas aeruginosa is a rod-shaped, Gram-negative, non-spore-forming, and motile bacterium possessing a single polar flagellum. It is widely recognized for its exceptional environmental resilience and metabolic versatility, which enable it to colonize a broad range of ecological niches, including soil, water, clinics, and hospital environments (1). A distinguishing feature of *P. aeruginosa* is its ability to grow at elevated temperatures

(up to 42°C), a trait not commonly observed among other *Pseudomonas* species (2-4). Clinically, it is a leading opportunistic pathogen responsible for a wide spectrum of infectious disorders, particularly in immunocompromised patients such as malignancies, severe burns, or those undergoing mechanical ventilation. It is also a major cause of chronic pulmonary infections in patients with cystic fibrosis (CF), chronic obstructive pulmonary disease (COPD), and bronchiectasis. The pathogen frequently colonizes the respiratory tract, bloodstream, urinary tract, and surgical sites, often resulting in severe clinical complications (5-7). The pathogenic role of *P. aeruginosa* is largely attributed to its intrinsic and acquired resistance mechanisms, including efflux pump overexpression, enzymatic degradation of antibiotics (β-lactamases), outer membrane permeability barriers, and its ability to form protective biofilms (8). These factors contribute to its inclusion in the ESKAPE group, a consortium of six nosocomial pathogens comprising *Enterococcus faecium*, *Staphylococcus aureus*, *Klebsiella pneumoniae*, *Acinetobacter baumannii*, *P. aeruginosa*, and *Enterobacter* species, identified by the Infectious Diseases Society of America (IDSA) for their notorious ability to evade standard antimicrobial therapies. Owing to its clinical burden and increasing resistance trends, the World Health Organization (WHO) has listed *P. aeruginosa* as a priority pathogen for the development of novel antimicrobials (9-12). According to the Centers for Disease Control and Prevention (CDC), multidrug-resistant *P. aeruginosa* was associated with an estimated 32,600 infections and approximately 2,700 deaths in hospitalized patients within the United States in 2017. On a global scale, antimicrobial resistance involving pathogens such as *P. aeruginosa* contributes to an estimated 700,000 to over 10 million deaths annually (13). This alarming scenario underscores the urgent need for innovative and effective preventive strategies, including the development of vaccines, to mitigate the healthcare impact of *P. aeruginosa* infections, especially among vulnerable patient populations (14).

Flagellin A, a surface-exposed and structurally conserved protein among *Pseudomonas aeruginosa* strains, represents a promising target for vaccine development due to its stability and immunological accessibility. It exists primarily in two forms, type A and type B differentiated by their molecular and serological properties, with type A displaying greater sequence variability (15). Notably, Flagellin A is capable of stimulating both innate and adaptive immune responses by engaging antigen-presenting cells and activating T lymphocytes. These immunostimulatory properties, combined with its widespread expression, make Flagellin A an ideal candidate for the construction of a multi-epitope peptide vaccine (16). Targeting this protein could lead to the development of an effective and durable immunization strategy, particularly beneficial for individuals at risk of recurrent or nosocomial *P. aeruginosa* infections (17, 18).

1. METHODOLOGY

2.1 Bacterial Antigenic Protein Sequence

The amino acid sequence of the bacterial Flagellin A protein was obtained from the UniProt database (https://www.uniprot.org). The sequence corresponding to the primary accession number P21184 was retrieved in FASTA format, comprising a total of 394 amino acids.

2.2 Antigenicity Assessment

To evaluate the antigenic potential of Flagellin A, its full-length amino acid sequence was analyzed using the VaxiJen server (version 2.0) available at https://www.ddg-pharmfac.net/vaxijen/VaxiJen/VaxiJen.html. The bacterial model was selected as the target organism, and a threshold of 0.5 was applied to distinguish probable antigens. To validate the findings and improve prediction reliability, the analysis was repeated using the updated VaxiJen v3.0 platform (https://www.ddg-pharmfac.net/vaxijen3/home).

2.3 Homology Analysis

To avoid cross-reactivity and potential autoimmune responses, the antigen sequence was compared against the human proteome. BLASTp searches were conducted using the NCBI BLAST server (https://blast.ncbi.nlm.nih.gov/Blast.cgi) with the search restricted to Homo sapiens (Taxonomy ID: 9606). This step aimed to identify any significant sequence similarity between Flagellin A and human proteins.

2.4 Prediction of Immune Cell Epitopes

2.4.1 B-cell Epitope

The B-cell linear epitopes of Flagellin A were predicted using the BepiPred Linear Epitope Prediction tool available through the Immune Epitope Database (IEDB) at http://tools.iedb.org/bcell. This method utilizes a combination of hidden Markov models and amino acid propensity scales to detect probable linear epitopes. Using this approach, 25 distinct B-cell epitopes were identified based on established threshold values.

1.4.2 Cytotoxic T Lymphocyte (CTL) Epitope

CTL epitopes were predicted using the Artificial Neural Network (ANN) 4.0 method accessible via the IEDB MHC class I prediction tool (https://nextgen-tools.iedb.org/pipeline?tool=tc1). This method estimates peptide binding affinities to a variety of MHC class I alleles.

1.4.3 Helper T Lymphocyte Epitope

Helper T-cell epitopes were predicted using the NN-align 2.3 method, part of the NetMHCII 2.3 suite (https://nextgen-tools.iedb.org/pipeline?tool=tc2). A peptide length of 15 amino acids was selected, and binding affinities were analyzed across 27 different MHC class II alleles. Both MHC class I and class II epitopes were selected based on their binding affinities expressed as IC50 values, where lower values indicate stronger predicted binding.

2.5 Antigenicity and Allergenicity Analysis of Predicted Epitopes

The antigenic potential of predicted epitopes including B-cell, cytotoxic T lymphocyte (CTL), and helper T lymphocyte (HTL) epitopes was assessed using **VaxiJen v2.0** (https://www.ddg-pharmfac.net/vaxijen/VaxiJen/VaxiJen.html). The bacterial model was selected as the target organism, with a threshold value set to 0.5. To enhance prediction reliability, cross-validation was performed using **VaxiJen v3.0** (https://www.ddg-pharmfac.net/vaxijen3/home). To determine the allergenicity of epitopes, the **AllerTOP v2.0** tool (https://www.ddg-pharmfac.net/allertop_test) was used. AllerTOP classifies protein sequences based on the Auto Cross-Covariance (ACC) transformation, converting variable-length sequences into fixed-length feature vectors. Only non-allergenic epitopes were selected for inclusion in the multi-epitope vaccine design to ensure safety.

2.6 Homology Analysis Against Human Proteins

To avoid autoimmune responses, the predicted epitopes were analyzed for sequence similarity against human proteins using the **BLASTp** algorithm (https://blast.ncbi.nlm.nih.gov/Blast.cgi?PROGRAM=blastp&PAGE_TYPE=BlastSearch&LINK_LOC=blasthome). The search was restricted to *Homo sapiens* (TaxID: 9606), and epitopes with significant similarity to human proteins were excluded.

2.7 Molecular Docking of Predicted Epitopes with MHC Molecules

Three MHC class I epitopes (ASLNTSLQR, ALNGEVKQL, AESLNGTYF) were selected based on immunogenicity and population coverage, and docked with HLA-A*02:03 (PDB ID: 3OX8), HLA-B*44:03 (PDB ID: 4JQX), and HLA-A*11:01 (PDB ID: 6ID4), respectively. For MHC class II, epitopes (TGVGTAAGVTPSATA, AVTAATASGTVDIAI) were selected and docked with the DQB1*03:01:01:01 allele. The allele sequence was obtained from the **IPD-IMGT/HLA database** (https://www.ebi.ac.uk/ipd/imgt/hla), translated to a protein sequence, and modeled using **AlphaFold v3** (https://alphafoldserver.com). Protein structures were prepared for docking by removing water molecules and ligands using **BIOVIA Discovery Studio Visualizer**. Molecular docking was carried out using the **HDOCK server** (http://hdock.phys.hust.edu.cn), which supports protein-protein docking.

2.8 Multi-Epitope Vaccine Construction

Eight multi-epitope vaccine constructs were designed by assembling predicted epitopes (6 B-cell, 14 MHC class I, and 10 MHC class II). Linkers (GPGPG, AAY) and appropriate adjuvants were included to enhance immunogenicity. Tertiary structures of each vaccine construct were modeled using **AlphaFold v3** (https://alphafoldserver.com).

2.9 Docking of Vaccine Constructs with Toll-like Receptors

Toll-like receptors **TLR5 (PDB ID: 3J0A)** and **TLR4 (PDB ID: 3FXI)** were downloaded from the Protein Data Bank. Docking was conducted using both the **HDOCK server** (http://hdock.phys.hust.edu.cn) and the **LZerD web server** (https://lzerd.kiharalab.org/upload) to assess interactions between the vaccine constructs and TLRs. A total of 16 docking runs were completed.

2.10 Evaluation of Antigenicity and Allergenicity of Construct

The construct showing the best docking results was further evaluated using **VaxiJen v2.0** and **v3.0** (https://www.ddg-pharmfac.net/vaxijen/VaxiJen/VaxiJen.html), and **AllerTOP v2.1** (https://www.ddg-pharmfac.net/allertop_test). These assessments ensured the selected construct was antigenic and non-allergenic.

2.11 Population Coverage Prediction

To estimate global applicability, population coverage was analyzed using the **IEDB Population Coverage Tool** (http://tools.iedb.org/population). A compiled list of selected MHC class I and II epitopes with corresponding HLA alleles was uploaded, and default parameters were used to estimate global coverage.

2.12 Secondary Structure and Structural Validation

Secondary structure was predicted using **PSIPRED** (http://bioinf.cs.ucl.ac.uk/psipred). Physicochemical parameters such as molecular weight, isoelectric point (pI), half-life, aliphatic index, and GRAVY were computed using **ProtParam** (https://web.expasy.org/protparam). The stereochemical quality of the vaccine model was evaluated by **MolProbity** (http://molprobity.biochem.duke.edu) using Ramachandran plot analysis.

2.13 Molecular Dynamics Simulation

Structural stability and flexibility of the final vaccine construct were assessed through **iMODS** (https://imods.iqfr.csic.es), which applies normal mode analysis (NMA) to simulate molecular dynamics and evaluate collective motions and deformability.

2.14 Codon Optimization and In Silico Cloning

Codon optimization for expression in *E. coli* K12 was conducted using **JCat** (https://www.jcat.de). The optimized nucleotide sequence was inserted into the **RepX_pET28a** plasmid vector using **Benchling** (https://www.benchling.com) for in silico cloning.

2.15 In Silico mRNA Transcription

The optimized DNA sequence was manually transcribed into mRNA by replacing thymine (T) with uracil (U). The resulting mRNA sequence was submitted to the **RNAfold web server** (http://rna.tbi.univie.ac.at/cgi-bin/RNAWebSuite/RNAfold) to predict its secondary structure and evaluate stability using minimum free energy (MFE) values.

2.16 3D mRNA Modeling and Ribosome Docking

The three-dimensional structure of the mRNA was predicted using **3dRNA** (http://biophy.hust.edu.cn/3dRNA). Docking analysis was performed between the mRNA and the **30S ribosomal subunit of** *E. coli* to evaluate its compatibility with the bacterial translation machinery.

2. RESULTS

3.1 Bacterial protein

The flagellin A protein of *Pseudomonas aeruginosa* was retrieved using the primary accession number P21184. This protein was selected due to its essential role as a structural component of the bacterial flagellum and its involvement in motility. The complete amino acid sequence, comprising 394 residues, was obtained in FASTA format for downstream computational analyses.

3.2 Antigenicity and homology analysis of the selected antigen

Antigenicity assessment was conducted using the bacterial model in the VaxiJen server, with a threshold set at 0.5. Flagellin A achieved an antigenic score of 0.7625, indicating a high probability of being an effective antigen. This result was further confirmed by VaxiJen v3.0, which predicted the protein as an immunogen with 100% probability. To minimize the

risk of host cross-reactivity, a sequence homology analysis was carried out by comparing the protein against the *Homo sapiens* proteome using BLASTp. The analysis revealed no significant similarity with any human proteins, indicating a low potential for autoimmune reactions and supporting its candidacy for vaccine development.

3.3 Immune cell epitope prediction

To identify immunologically active regions within the flagellin A sequence, both B-cell and T-cell epitopes were predicted using immune-informatics tools. A total of 25 linear B-cell epitopes were identified using the BepiPred prediction method (**Figure 1**). These regions are likely to be surface-accessible and recognized by antibodies. In the BepiPred output, yellow-highlighted segments represent sequences with scores above the prediction threshold, indicating a high probability of epitope presence. Green regions fall below the threshold and are considered less likely to be antigenic. The average prediction score was 0.375, with a minimum of -0.013 and a maximum of 2.000.Cytotoxic T lymphocyte (CTL) epitopes were predicted based on their binding affinity to MHC class I molecules, with only epitopes showing IC50 values of ≤100 nM retained for further analysis. This screening identified 58 high-affinity MHC class I epitopes. For helper T lymphocyte (HTL) epitopes, predictions were performed using the same IC50 threshold of ≤100 nM, resulting in 68 strong-binding MHC class II epitopes suitable for inclusion in the multi-epitope vaccine construct.

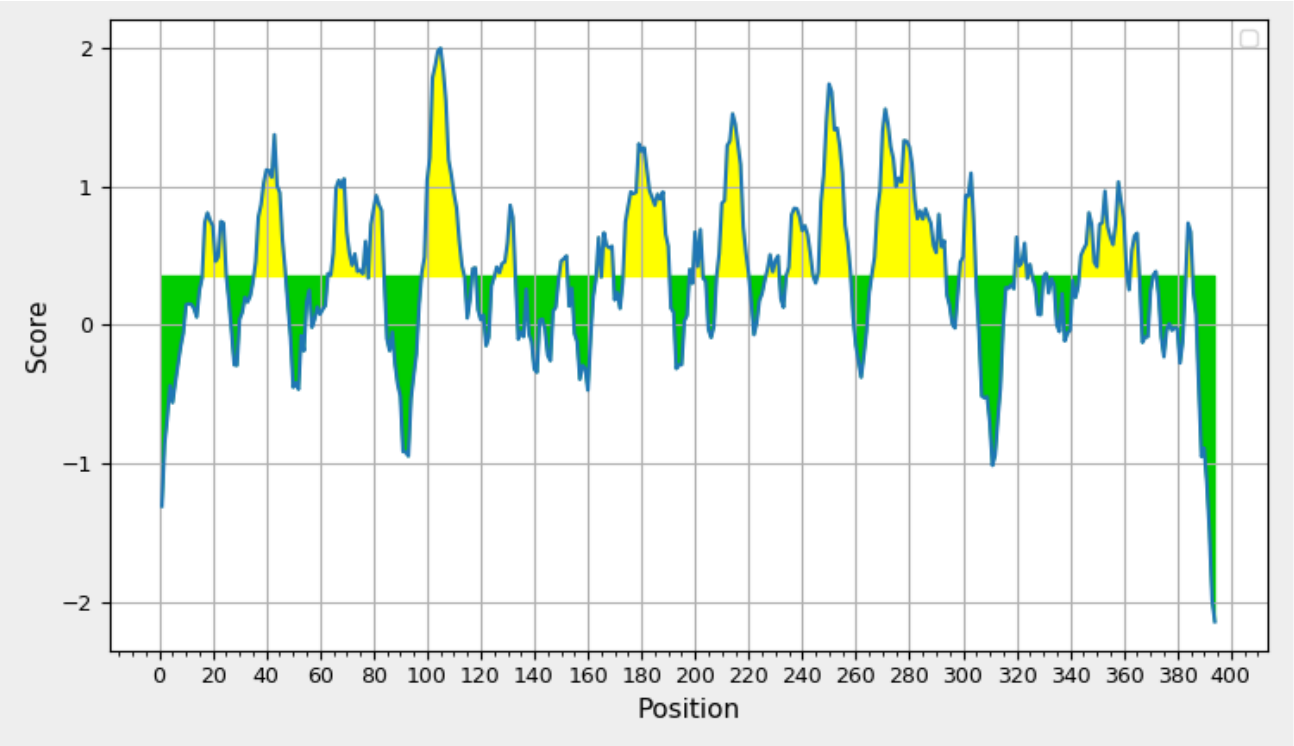

Figure 1. B-cell epitope prediction of flagellin A using the IEDB BepiPred tool

2.4 Antigenicity and Allergenicity Analysis of Predicted Immune Cell Epitopes

The predicted B-cell and T-cell epitopes (MHC class I and II) were evaluated for their antigenic potential using the VaxiJen v2.0 server, with a threshold set at 0.5 and were classified as probable antigens. Out of the 25 predicted B-cell epitopes, 9 exceeded the antigenicity threshold, confirming their potential to induce a strong immune response. The antigenic B-cell epitopes are listed in **Table 1**.

Table 1. Antigenicity assessment of selected B-cell epitopes predicted from the flagellin A protein using VaxiJen v2.0.

Epitope Sequence	Antigenic Score	Prediction
NLNNSSASL	0.7608	Probable Antigen
SRINSAKDDAAG	1.2264	Probable Antigen
VATKNANDGISLAQT	0.6209	Probable Antigen
QSANGSNSDSERTALN	1.8258	Probable Antigen
FKADGGGAVTAATASGT	1.5501	Probable Antigen
MKGNETAEQAAA	1.3611	Probable Antigen
SKAGKDGSGAITS	1.9490	Probable Antigen
ADTGSTGVGTAAGVTPSATAFAKTNDTV	1.2219	Probable Antigen
ENVSAARGRIEDTDFAAE	0.8987	Probable Antigen

The antigenic epitopes identified from B-cell and T-cell predictions were further evaluated for allergenicity using the AllerTOP v2.1 server. Among the B-cell epitopes, 6 were found to be non-allergenic while retaining their antigenic properties (**Table 2**). For the T-cell epitopes, 14 MHC-I and 10 MHC- II epitopes were both antigenic and non-allergenic, indicating their safety and feasibility for inclusion in the vaccine design. All listed epitopes were classified as immunogenic and non-allergenic.

Table 2. B-cell epitopes analysis using VaxiJen v2.0 and allergenicity using AllerTOP v2.1.

Epitope	Antigenicity Score	Antigenicity	Allergenicity
NLNNSSASL	0.7608	Immunogen	Non-allergen
SRINSAKDDAAG	1.2264	Immunogen	Non-allergen
VATKNANDGISLAQT	0.6209	Immunogen	Non-allergen
QSANGSNSDSERTALN	1.8258	Immunogen	Non-allergen
MKGNETAEQAAA	1.3611	Immunogen	Non-allergen
ENVSAARGRIEDTDFAAE	0.8987	Immunogen	Non-allergen

For CTL epitope evaluation, 30 MHC class I epitopes were identified as antigenic using the same 0.5 threshold in VaxiJen v2.0. Of these, 14 epitopes were confirmed to be non-allergenic upon analysis with AllerTOP v2.1 as listed in Table 3. Their ability to elicit a strong immune response without causing allergenic reactions supports their inclusion in the vaccine design. Similarly, HTL epitopes 25 MHC class II epitopes displayed antigenicity above the threshold and were further assessed for allergenic potential. Out of these, 10 epitopes were found to be non-allergenic (**Table 3**). These HTL epitopes not only possess strong immunogenic potential but also exhibit safety characteristics, indicating their value in eliciting a robust and balanced immune response.

Table 3. List of selected T-cell epitopes (MHC class I and II) from flagellin A, evaluated for antigenicity and allergenicity

Epitope	Class	Antigenicity Score	Antigenicity	Allergenicity
KLLDGSFGV	MHC I	0.5703	Immunogen	Non-allergen

NIASLNTQR	MHC I	0.6453	Immunogen	Non-allergen
TAATASGTV	MHC I	1.2641	Immunogen	Non-allergen
SLNTSLQRL	MHC I	0.6747	Immunogen	Non-allergen
NLNNSSASL	MHC I	0.7608	Immunogen	Non-allergen
SLNGTYFKA	MHC I	1.1093	Immunogen	Non-allergen
AAAKIAAAV	MHC I	0.5459	Immunogen	Non-allergen
AESLNGTYF	MHC I	0.8591	Immunogen	Non-allergen
ASLNTSLQR	MHC I	0.7014	Immunogen	Non-allergen
ATKNANDGI	MHC I	0.6481	Immunogen	Non-allergen
AIKQIDAQR	MHC I	0.6733	Immunogen	Non-allergen
KTNDTVAKI	MHC I	1.0513	Immunogen	Non-allergen
ALNGEVKQL	MHC I	1.0889	Immunogen	Non-allergen
TVAKIDIST	MHC I	0.7896	Immunogen	Non-allergen
TGVGTAAGVTPSATA	MHC II	1.3106	Immunogen	Non-allergen
NTSLQRLSTGSRINS	MHC II	0.7156	Immunogen	Non-allergen
AVTAATASGTVDIAI	MHC II	1.2074	Immunogen	Non-allergen
NTNIASLNTQRNLNN	MHC II	0.5575	Immunogen	Non-allergen
IDEAIKQIDAQRADL	MHC II	0.6565	Immunogen	Non-allergen
RLSTGSRINSAKDDA	MHC II	0.9264	Immunogen	Non-allergen
GNETAEQAAAKIAAA	MHC II	1.1986	Immunogen	Non-allergen
SKAGKDGSGAITSAV	MHC II	1.6622	Immunogen	Non-allergen
KLLDGSFGVASFQVG	MHC II	0.7707	Immunogen	Non-allergen
SLNTQRNLNNSSASL	MHC II	0.6478	Immunogen	Non-allergen

3.5 Human homology analysis of predicted epitopes

All selected B and T-cell (MHC I and II) epitopes were analyzed for similarity against the Homo sapiens proteome. The results showed no significant sequence similarity with human proteins, indicating minimal risk of cross-reactivity or induction of autoimmune responses. This supports the safety of these epitopes for further evaluation as vaccine candidates.

3.6 Molecular docking results of T-cell epitopes with MHC molecules

The predicted T-cell epitopes demonstrated favorable binding affinities with their respective MHC alleles. Among the MHC class I epitopes, ASLNTSLQR exhibited the strongest binding with HLA-A*11:01 (PDB ID: 6ID4), with a docking score of −189.76. AESLNGTYF showed moderate interaction with HLA-B*44:03 (PDB ID: 4JQX), while ALNGEVKQL had the lowest docking score of −146.45 with HLA-A*02:03 (PDB ID: 3OX8). In MHC class II, all three selected epitopes interacted with DQB1*03:01:01:01. SKAGKDGSGAITSAV displayed the highest binding affinity with a docking score of −193.60, followed by TGVGTAAGVTPSATA with −187.46 and AVTAATASGTVDIAI with −181.60. These strong interactions suggest that the epitopes possess significant immunogenic potential and could serve as promising candidates in vaccine design. The docking results for six selected T-cell epitopes revealed distinct binding affinities with their respective MHC molecules. Among the MHC class I epitopes, ASLNTSLQR showed the strongest interaction with HLA-A*11:01, as indicated by a docking score of −189.76. AESLNGTYF demonstrated moderate binding with HLA-B*44:03 (−158.32), whereas ALNGEVKQL exhibited the weakest interaction with HLA-A*02:03 (−146.45). For MHC class II, all three epitopes were docked with DQB1*03:01:01:01. The epitope SKAGKDGSGAITSAV had the highest binding affinity (−193.60), followed by TGVGTAAGVTPSATA (−187.46), and AVTAATASGTVDIAI showed the lowest (−181.60). These results suggest strong potential immunogenicity

of the selected epitopes for further evaluation in vaccine design (**Table 4**).

Table 4. Docking scores of predicted T-cell epitopes with MHC class I and II alleles

Epitope Type	Epitope Sequence	MHC Allele	PDB ID	Docking Score (kcal/mol)	Binding Affinity
MHC I	ASLNTSLQR	HLA-A*11:01	6ID4	−189.76	Strong
MHC I	AESLNGTYF	HLA-B*44:03	4JQX	−158.32	Moderate
MHC I	ALNGEVKQL	HLA-A*02:03	3OX8	−146.45	Lowest
MHC II	SKAGKDGSGAITSAV	DQB1*03:01:01:01	–	−193.60	Strong
MHC II	TGVGTAAGVTPSATA	DQB1*03:01:01:01	–	−187.46	Moderate
MHC II	AVTAATASGTVDIAI	DQB1*03:01:01:01	–	−181.60	Lowest

3.7 Multiple Vaccine Constructs Development

Following the antigenicity and allergenicity assessment of the predicted epitopes, a total of 6 B-cell epitopes, 14 MHC class I epitopes, and 10 MHC class II epitopes were identified. Due to the potential issues associated with incorporating a large number of epitopes such as increased molecular weight and improper protein folding, eight multiepitope vaccine constructs were developed (20). These constructs differed in epitope arrangement and combination, aiming to identify the most stable and immunologically favorable candidate. Each construct was engineered by integrating appropriate adjuvants, T-cell and B-cell epitopes, and linkers to maintain structural flexibility and functional separation, and C-terminal histidine tags to enable downstream purification. Strategic variation in the positioning of epitopes was applied to influence the structural conformation of the final vaccine product, potentially altering its interaction with immune receptors (4). All eight vaccine sequences were subjected to 3D structure prediction using AlphaFold v3. The structural models were generated successfully and stored for subsequent structural validation and analysis. The detailed sequences of the eight constructs are provided in **Table 5**.

Table 5. Final Vaccine Constructs Designed Using Predicted Epitopes, Linkers, and Adjuvant Sequences.

Construct No.	Vaccine Construct (Sequence)
Construct 1	MQTIIPSTDQNAVQSINTEHATAIFVAGEAAAKTAATASGTVAAYSLNGT YFKAAAYALNGEVKQLAAYKTNDTVAKIAAYAESLNGTYFAAYTVAKIDI STAAYNLNNSSASLAAYASLNTSLQRGPGPGSKAGKDGSGAITSAVGPGP GTGVGTAAGVTPSATAGPGPGAVTAATASGTVDIAIGPGPGGNETAEQ AAAKIAAAGPGPGRLSTGSRINSAKDDAGPGPGKLLDGSFGVASFQVGG PGPGNTSLQRLSTGSRINSKKQSANGSNSDSERTALNKKMKGNETAEQA AAKSRINSAKDDAAGKKENVSAARGRIEDTDFAAEKKNLNNSSASLHHH HHH
Construct 2	MQTIIPSTDQNAVQSINTEHATAIFVAGEAAAKSLNGTYFKAAAYALNGE VKQLAAYKTNDTVAKIAAYAESLNGTYFAAYTVAKIDISTAAYNLNNSSA SLAAYASLNTSLQRAAYTAATASGTVGPGPGSKAGKDGSGAITSAVGPG PGTGVGTAAGVTPSATAGPGPGAVTAATASGTVDIAIGPGPGGNETAE QAAAKIAAAGPGPGRLSTGSRINSAKDDAGPGPGKLLDGSFGVASFQVG GPGPGNTSLQRLSTGSRINSKKMKGNETAEQAAAKSRINSAKDDAAGKK ENVSAARGRIEDTDFAAEKKNLNNSSASLKKQSANGSNSDSERTALNHH HHHH

Construct 3	MQTIIPSTDQNAVQSINTEHATAIFVAGEAAAKTAATASGTVAAYSLNGT YFKAAAYALNGEVKQLAAYKTNDTVAKIAAYAESLNGTYFAAYTVAKIDI STAAYNLNNSSASLAAYASLNTSLQRGPGPGTGVGTAAGVTPSATAGPG PGAVTAATASGTVDIAIGPGPGGNETAEQAAAKIAAAGPGPGRLSTGSRI NSAKDDAGPGPGKLLDGSFGVASFQVGGPGPGNTSLQRLSTGSRINSGP GPGSKAGKDGSGAITSAVKKQSANGSNSDSERTALNKKMKGNETAEQA AAKSRINSAKDDAAGKKENVSAARGRIEDTDFAAEKKNLNNSSASLHHH HHH
Construct 4	MQTIIPSTDQNAVQSINTEHATAIFVAGEAAAKTAATASGTVAAYSLNGT YFKAAAYALNGEVKQLAAYKTNDTVAKIAAYAESLNGTYFAAYTVAKIDI STAAYNLNNSSASLAAYASLNTSLQRGPGPGSKAGKDGSGAITSAVGPGP GTGVGTAAGVTPSATAGPGPGAVTAATASGTVDIAIGPGPGGNETAEQ AAAKIAAAGPGPGRLSTGSRINSAKDDAGPGPGKLLDGSFGVASFQVGG PGPGNTSLQRLSTGSRINSKKMKGNETAEQAAAKSRINSAKDDAAGKKE NVSAARGRIEDTDFAAEKKNLNNSSASLKKQSANGSNSDSERTALNHHH HHH
Construct 5	MQTIIPSTDQNAVQSINTEHATAIFVAGEAAAKASLNTSLQRAAYNLNNS SASLAAYTVAKIDISTAAYAESLNGTYFAAYKTNDTVAKIAAYALNGEVK QLAAYSLNGTYFKAAAYTAATASGTVGPGPGSKAGKDGSGAITSAVGPG PGTGVGTAAGVTPSATAGPGPGAVTAATASGTVDIAIGPGPGGNETAE QAAAKIAAAGPGPGRLSTGSRINSAKDDAGPGPGKLLDGSFGVASFQVG GPGPGNTSLQRLSTGSRINSKKENVSAARGRIEDTDFAAEKKSRINSAKD DAAGKKMKGNETAEQAAAKQSANGSNSDSERTALNKKNLNNSSASLH HHHHH
Construct 6	MQTIIPSTDQNAVQSINTEHATAIFVAGEAAAKTAATASGTVAAYSLNGT YFKAAAYALNGEVKQLAAYKTNDTVAKIAAYAESLNGTYFAAYTVAKIDI STAAYNLNNSSASLAAYASLNTSLQRGPGPGNTSLQRLSTGSRINSGPGP GKLLDGSFGVASFQVGGPGPGRLSTGSRINSAKDDAGPGPGGNETAEQ AAAKIAAAGPGPGAVTAATASGTVDIAIGPGPGTGVGTAAGVTPSATAG PGPGSKAGKDGSGAITSAVKKQSANGSNSDSERTALNKKMKGNETAEQ AAAKSRINSAKDDAAGKKENVSAARGRIEDTDFAAEKKNLNNSSASLHH HHHH
Construct 7	MQTIIPSTDQNAVQSINTEHATAIFVAGEAAAKSKAGKDGSGAITSAVGP GPGTGVGTAAGVTPSATAGPGPGAVTAATASGTVDIAIGPGPGGNETA EQAAAKIAAAGPGPGRLSTGSRINSAKDDAGPGPGKLLDGSFGVASFQV GGPGPGNTSLQRLSTGSRINSGPGPGSLNGTYFKAAAYALNGEVKQLAA YKTNDTVAKIAAYAESLNGTYFAAYTVAKIDISTAAYNLNNSSASLAAYTA ATASLNTSLQRAAYTAATASGTVKKQSANGSNSDSERTALNKKMKGNE TAEQAAAKSRINSAKDDAAGKKENVSAARGRIEDTDFAAEKKNLNNSSA SLHHHHHH
Construct 8	MQTIIPSTDQNAVQSINTEHATAIFVAGEAAAKALNGEVKQLAAYTVAKI DISTAAYSLNGTYFKAAAYASLNTSLQRAAYKTNDTVAKIAAYAESLNGT YFAAYTAATASGTVAAYNLNNSSASLGPGPGAVTAATASGTVDIAIGPGP GSKAGKDGSGAITSAVGPGPGNTSLQRLSTGSRINSGPGPGTGVGTAAG VTPSATAGPGPGGNETAEQAAAKIAAAGPGPGRLSTGSRINSAKDDAGP GPGKLLDGSFGVASFQVGKKENVSAARGRIEDTDFAAEKKSRINSAKDD

	AAGKKMKGNETAEQAAAKQSANGSNSDSERTALNKKNLNNSSASLHH HHHH

3.8 Docking Analysis of Vaccine Constructs

Molecular docking was conducted to assess the binding interactions between the designed multi-epitope vaccine constructs and Toll-like receptors TLR4 and TLR5 using the HDOCK server. As summarized in **Table 6**, all eight constructs exhibited favorable docking scores, confidence values, and ligand RMSD, indicating strong interaction potential. Among these, Construct 7 demonstrated the most favorable binding with TLR4, achieving a docking score of –325.83, the highest confidence score (0.9712), and a relatively low ligand RMSD of 91.11 Å. Its docking with TLR5 also showed strong interaction, with a score of –307.39 and a confidence value of 0.9588, suggesting stable and specific interactions with both receptors.

Table 6. Molecular Docking Results of Vaccine Constructs with TLR4 and TLR5 Using the HDOCK Server

Construct	Receptor	Docking Score	Confidence Score	Ligand RMSD (Å)	Construct	Receptor	Docking Score	Confidence Score	Ligand RMSD (Å)
1	TLR5	–312.55	0.9627	230.09	5	TLR5	–318.79	0.9669	320.43
1	TLR4	–254.69	0.8903	122.64	5	TLR4	–252.16	0.8853	221.39
2	TLR5	–287.43	0.9398	237.63	6	TLR5	–356.20	0.9841	179.94
2	TLR4	–286.37	0.938	99.54	6	TLR4	–280.24	0.9312	57.39
3	TLR5	–298.84	0.9515	146.63	7	TLR5	–307.39	0.9588	202.79
3	TLR4	–265.74	0.9101	86.44	7	TLR4	–325.83	0.9712	91.11
4	TLR5	–333.39	0.9751	236.41	8	TLR5	–301.31	0.9537	217.48
4	TLR4	–310.11	0.9609	94.24	8	TLR4	–267.30	0.9126	131.49

To validate these findings, the LZerD server was employed as a cross-docking platform, which uses three scoring functions GOAP, DFIRE, and ITScore to evaluate docking performance. Each docking complex was assigned a rank based on these metrics, and a rank-sum score was calculated to provide an overall assessment (**Table 7**). Construct 5 achieved the lowest rank sum (14) for TLR5, indicating excellent compatibility, while Construct 6 followed closely with a score of 18. Notably, Construct 7 ranked among the top candidates for both TLR4 (rank sum 61) and TLR5 (rank sum 39), showing consistent performance across both receptors. The GOAP score (–220,664.25) and DFIRE score (–162,620.49) for Construct 7 with TLR4 support its strong binding affinity, in agreement with HDOCK results. The consistency across two independent docking platforms highlights Construct 7 as the most promising vaccine candidate. The 3D structural models of vaccine constructs 7 and 8 complexes with TLR4 and TLR5 are illustrated in **Figure 2**, further supporting the stability of these interactions and justifying further evaluation through structural refinement and experimental validation

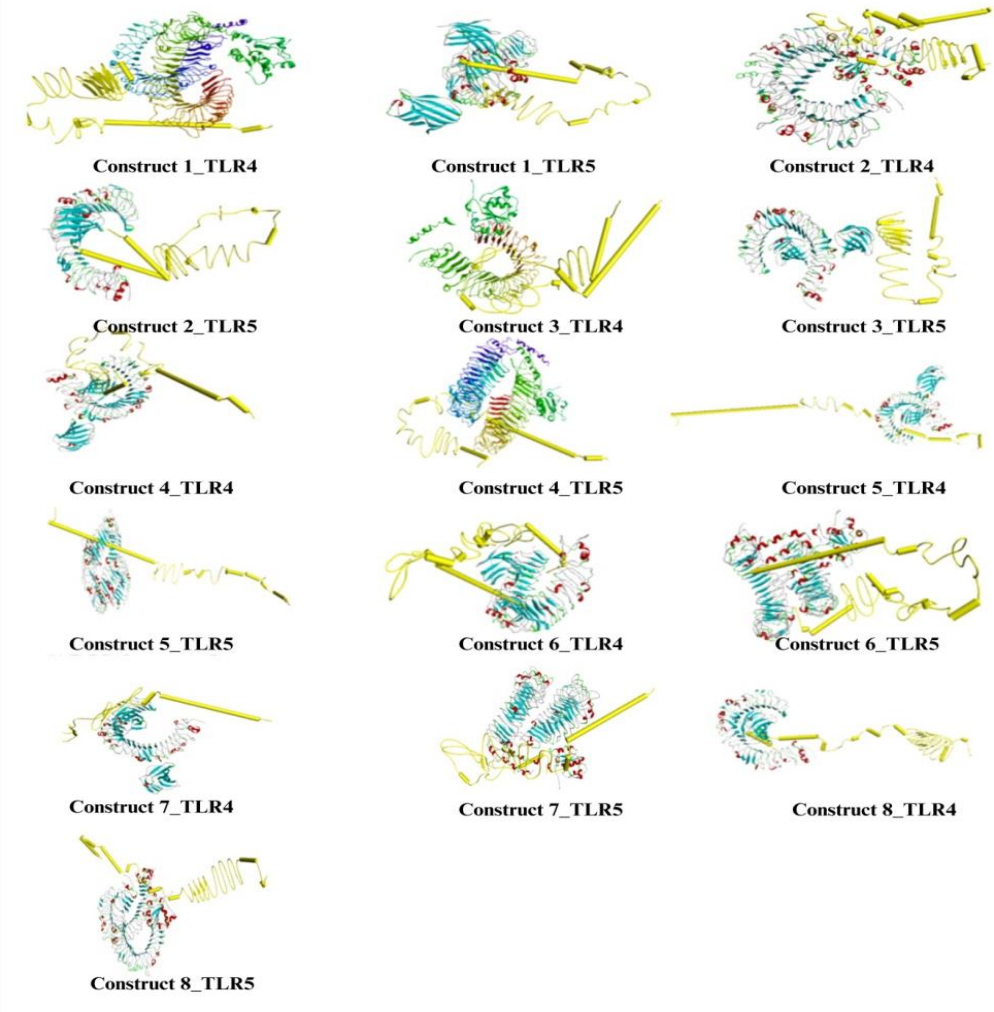

Figure 2. Molecular docking interactions of vaccine constructs (1–8) with TLR4 and TLR5 receptors, predicted using the HDOCK server.

Table 7. LZerD Server-Based Docking Evaluation of Vaccine Constructs with TLR4 and TLR5

Construct	Receptor	GOAP Score	GOAP Rank	DFIRE Score	DFIRE Rank	IT Score	IT Rank	Sum Score
1	TLR5	−143284.85	44	−141647.91	4	−65769.12	2	50
1	TLR4	−222554.51	179	−164805.97	16	−79966.70	8	203
2	TLR5	−146554.64	6	−141866.07	106	−66229.66	21	133
2	TLR4	−225138.36	123	−165137.41	209	−80499.40	18	350
3	TLR5	−144926.31	18	−141832.65	81	−66100.21	43	142

3	TLR4	−224172.44	256	−165267.10	71	−80337.20	79	406
4	TLR5	−143561.32	24	−140975.48	6	−65631.45	3	33
4	TLR4	−222700.84	154	−163834.88	96	−79611.11	45	295
5	TLR5	−142348.40	4	−140529.63	6	−66602.45	4	14
5	TLR4	−220967.32	34	−163574.14	38	−80727.09	21	93
6	TLR5	−144466.12	6	−141538.25	6	−65996.37	6	18
6	TLR4	−223796.93	7	−164412.51	50	−80193.83	8	65
7	TLR5	−140737.43	31	−139592.85	5	−64876.54	3	39
7	TLR4	−220664.25	13	−162620.49	22	−78925.86	26	61
8	TLR5	−144397.89	10	−141145.31	45	−65470.17	12	67
8	TLR4	−223746.05	52	−164458.24	47	−79616.82	37	136

3.9 Antigenicity and Allergenicity Analysis of Selected Vaccine Candidate

The immunogenicity and allergenicity of the designed vaccine construct were thoroughly assessed (**Table 8**). VaxiJen v2.0 predicted a high antigenicity score of 1.0249, while VaxiJen v3.0 further validated its immunogenic nature by identifying the construct as 100% immunogenic. Allergenicity analysis using AllerTop v2.1 classified the construct as non-allergenic, indicating minimal risk of allergic reactions. These results collectively highlight the construct's potential for safe and effective immune stimulation, supporting its candidacy for future in vivo evaluation. To enhance innate immune activation, the N-terminal D0 domain of Flagellin A (28 amino acids), a known TLR5 agonist, was integrated as an adjuvant. A rigid EAAAK linker was used to separate the adjuvant from downstream epitope regions, promoting structural stability and proper folding. The construct consists of epitope blocks targeting HTL, CTL, and B cells. These blocks are connected by specific linkers, GPGPG for HTL, AAY for CTL, and KK for B-cell epitopes ensuring functional separation and optimal immune recognition. A 6×His purification tag was added at the C-terminal end to facilitate downstream purification processes.

Table 8. Structural Composition of the Final Vaccine Construct.

Component	Description	Component	Description
Adjuvant	Flagellin A partial (28 aa, TLR5 agonist)	CTL Block	8 epitopes, joined by AAY linkers
Linker	EAAAK (rigid separator)	Spacer Linker	KK (precedes B-cell block)
HTL Block	7 epitopes, joined by GPGPG linkers	B-cell Block	5 epitopes, joined by KK linkers

Spacer Linker	GPGPG (extra, as in original FASTA)	Purification Tag	6×His (HHHHHH)

3.10 Population coverage analysis

For assessing the global immunological reach of the selected epitopes, population coverage analysis was conducted using the IEDB population coverage tool (**Figure 3**). The combined MHCI and II binding data revealed a global coverage of 62.54%, suggesting that a significant proportion of the global population would be capable of mounting an immune response to the vaccine. On average, 1.1 epitope-HLA combinations were recognized per individual, indicating that most individuals are likely to respond to at least one epitope included in the construct. The PC90 value, representing the number of epitope hits recognized by 90% of the population, was calculated to be 0.27, reflecting moderate but broad-spectrum immune coverage.

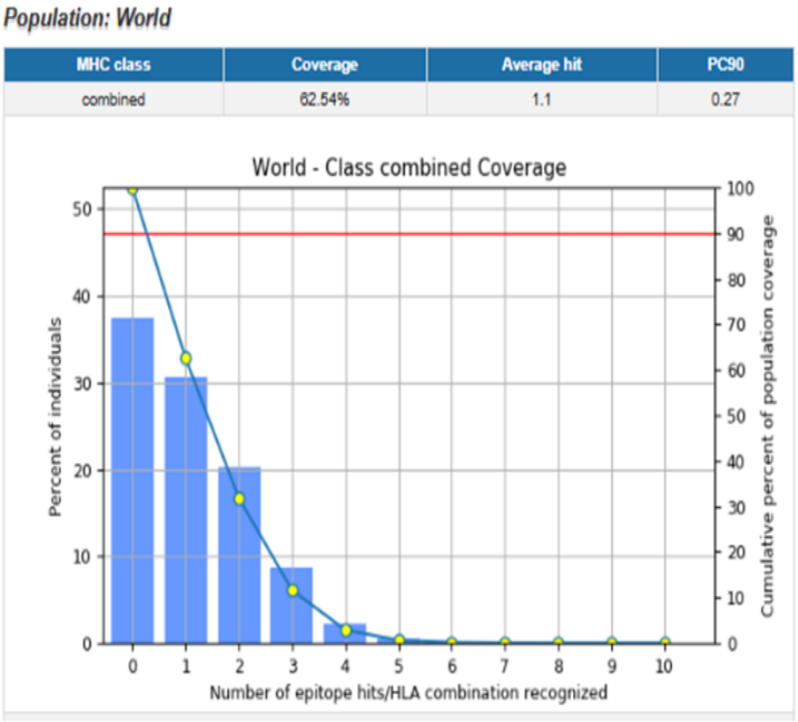

Figure 3. Cumulative curve illustrates a moderate yet widespread immune responsiveness across diverse populations.

3.11 Vaccine secondary structure prediction and structural evaluation

To analyze the structural properties of the selected vaccine (Construct 7), the PSIPRED Protein Structure Prediction Server was employed. The results indicated a predominance of alpha-helices and random coils, suggesting a stable conformation with flexible regions (**Figure 4**). Additionally, short segments of beta strands were observed, contributing to the overall structural integrity of the construct. This distribution of secondary elements supports the proper exposure and maintenance of conformational epitopes, essential for eliciting a strong immune response.

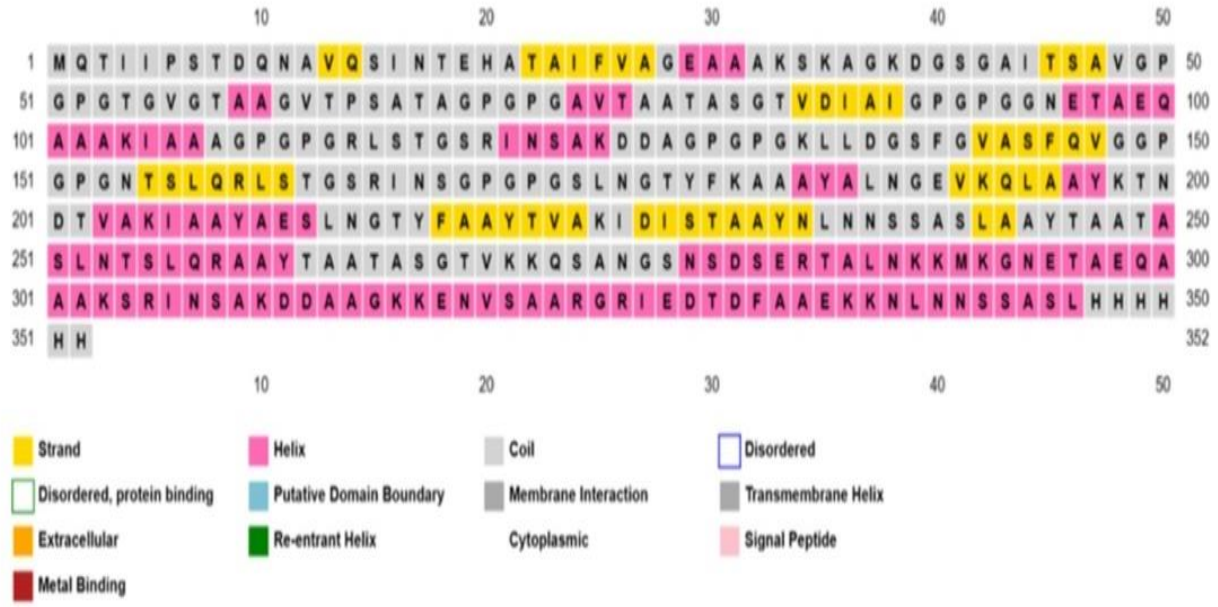

Figure 4. Predicted secondary structure showing abundant alpha-helices and random coils, with occasional beta strands indicating areas of structural rigidity.

To further assess the quality of the predicted tertiary structure, Ramachandran plot analysis was conducted using the PROCHECK server. The analysis demonstrated that the majority of residues were located in the most favored and additionally allowed regions, indicating good stereochemical quality. A minimal number of residues were found in disallowed regions, mainly involving flexible amino acids such as glycine and proline, which is acceptable in protein modeling. The distribution of phi (φ) and psi (ψ) dihedral angles aligns well with high-resolution protein structures, confirming that Construct 7 exhibits proper folding and structural stability, suitable for further molecular and functional analyses. The Ramachandran plot illustrates the phi (φ) and psi (ψ) angle distribution of residues such as alanine (Ala), arginine (Arg), asparagine (Asn), aspartic acid (Asp), glycine (Gly), and others within the vaccine construct (**Figure 5**). Most residues are concentrated within the favored regions, indicating correct stereochemical geometry. A few outliers, such as A250 and A227, suggest minor local torsional strain; however, these deviations are within acceptable limits and do not compromise the overall structural stability of the protein.

Figure 6 illustrates the φ and ψ angle distribution of residues including isoleucine, leucine, lysine, methionine, phenylalanine, proline, serine, and threonine. The majority of these residues are located within the most favored and additionally allowed regions of the Ramachandran plot, indicating a well-folded protein structure with minimal conformational strain. A limited number of outliers, such as A121 and A251, suggest acceptable local flexibility. Isolated deviations like A179 and A270 were observed but do not compromise the overall structural integrity. These findings confirm that the model demonstrates high stereochemical quality and proper folding. ERRAT analysis of Construct 7 yielded a high overall quality factor of 98.27, reflecting excellent reliability of non-bonded atomic interactions. This result supports the structural accuracy of the modeled vaccine and affirms its suitability for downstream computational analyses, such as molecular docking or simulation studies.

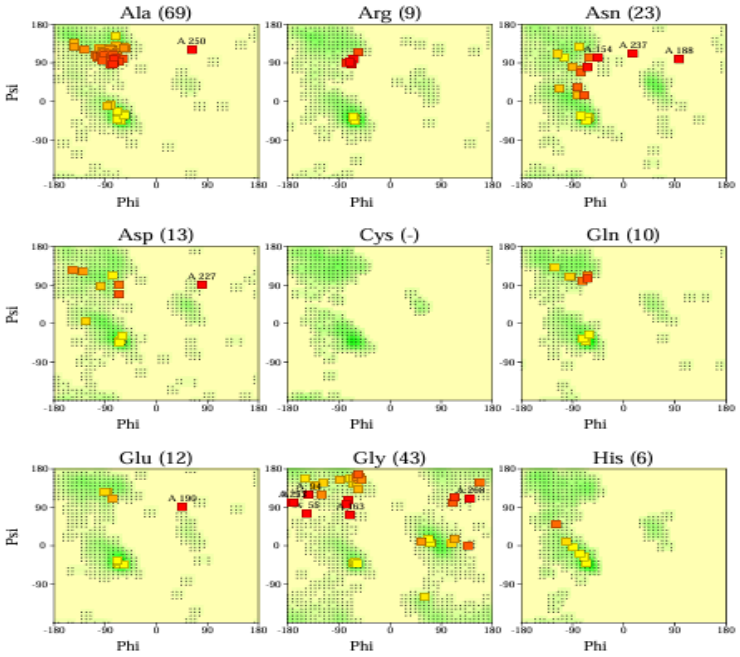

Figure 5. The Ramachandran plot illustrates the φ-ψ angle distribution of residues.

The physicochemical profile of the vaccine construct was assessed using the ProtParam tool. An instability index of 14.65 was recorded, which is well below the threshold value of 40, indicating strong structural stability for potential expression in heterologous systems. The negative GRAVY score of –0.352 confirms a hydrophilic nature, favoring aqueous solubility and enhancing immunogenic accessibility. A theoretical isoelectric point (pI) of 9.28 suggests that the protein may exhibit strong electrostatic interactions with negatively charged host membranes. The absence of cysteine residues eliminates the risk of inappropriate disulfide bond formation, further simplifying the folding process. Predicted half-lives exceeding 10 hours in *E. coli*, 20 hours in yeast, and 30 hours in mammalian cells further underscore the vaccine's potential for high-yield expression. Collectively, these properties highlight the construct's robustness and compatibility for experimental validation.

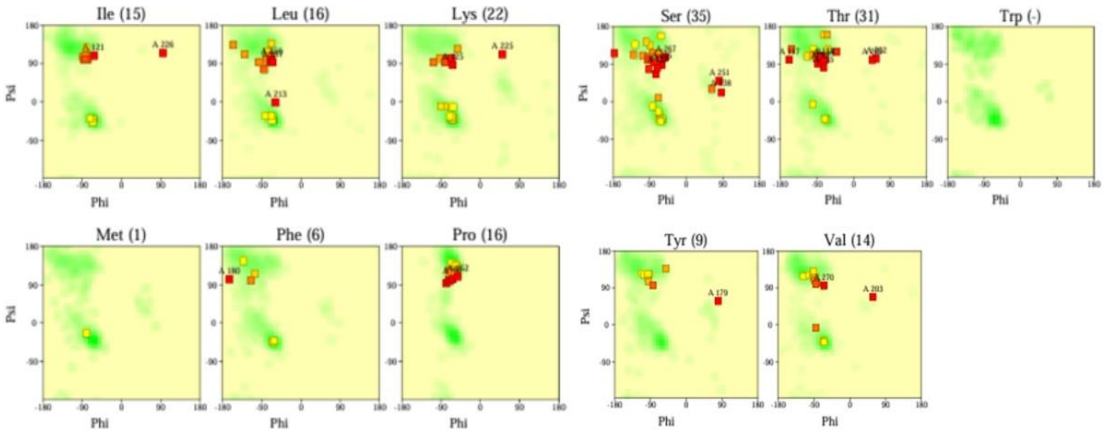

Figure 6. Illustration of the φ (phi) and ψ (psi) angle distribution of residues by Ramachandran Plot

3.12 Immune Simulation

To evaluate the immunological performance of the vaccine construct, an immune simulation was conducted using the C-ImmSim platform. The simulation results demonstrated a strong and coordinated activation of both humoral and cellular immune responses. An initial surge in IgM levels was followed by a consistent rise in IgG antibodies, reflecting the establishment of long-term immunological memory. Repeated stimulation of B lymphocytes and both CD4+ and CD8+ T lymphocytes was observed, suggesting successful immune priming. The vaccine construct also induced elevated interleukin-2 (IL-2) levels, indicating enhanced T-cell proliferation and differentiation. A gradual reduction in antigen levels over the course of the simulation confirmed efficient antigen clearance by the immune system. The predicted epitopes exhibited strong binding affinities for multiple MHC class I and II alleles, suggesting their ability to be broadly recognized across diverse genetic backgrounds. **Figure 8a** illustrates the kinetics of antigen concentration and antibody production following vaccine administration. A robust IgM response is evident early on, transitioning into sustained IgG production, characteristic of effective adaptive immunity. **Figure 8b** presents the cytokine profile over a 35-day period, highlighting peaks of IFN-γ and IL-2 around day 5, indicating early and potent T-cell activation. Additional cytokines such as IL-6, IL-12, and TNF-α showed moderate yet supportive responses. The inset within the figure emphasizes the dynamic changes in IL-2 expression, which correlate with the expansion of memory T-cell populations.

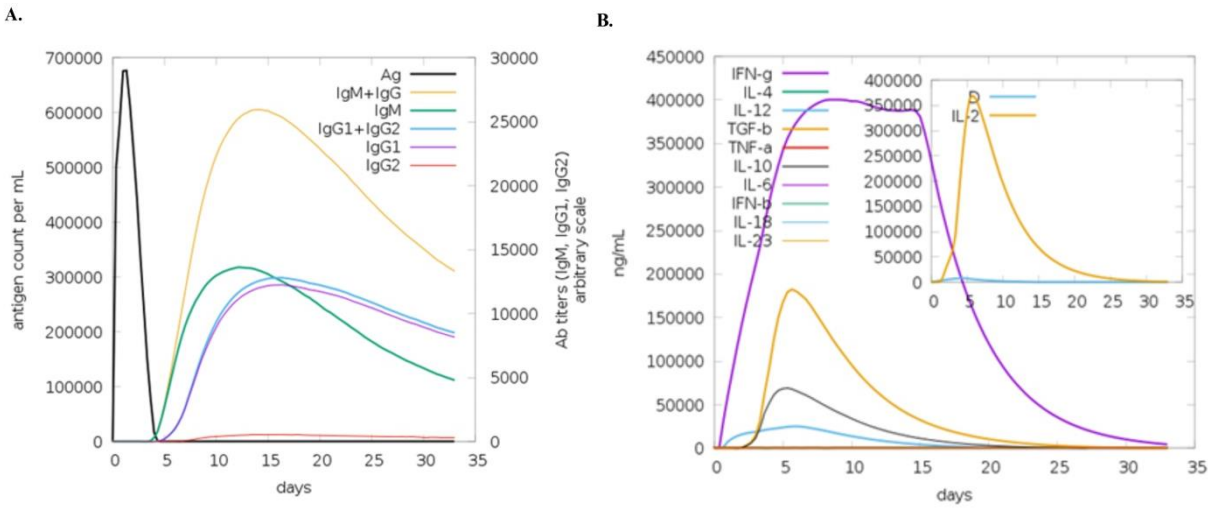

Figure 8. A. Antigen clearance (black) and antibody kinetics over 35 days, showing an early IgM peak followed by sustained IgG1 and IgG2 responses, indicative of effective humoral immunity.
B. Cytokine dynamics over 35 days, with IFN-γ and IL-2 peaking early to signal strong T-cell activation, alongside moderate IL-6, IL-10, IL-12 and TNF-α levels that support a balanced immune response.

3.13 Molecular Dynamics Simulation

Normal Mode Analysis (NMA) conducted through the iMODS server revealed notable flexibility in the vaccine construct, particularly within its terminal and loop regions. Theoretical B-factor values obtained from the simulation showed strong agreement with experimental data, reinforcing the accuracy of the dynamic model. Areas displaying higher deformability likely represent hinge-like motions, essential for structural rearrangements during antigen presentation. The dominance of low-frequency modes suggests the presence of large-scale, energetically favorable collective motions relevant to biological function. The eigenvalue analysis further supports this, indicating that these modes require minimal energy to activate. Correlation maps highlighted strong atomic interactions along the diagonal, reflecting coordinated movements among

neighboring residues. Additionally, significant long-range correlations between residues 1–100 and 200–320 point toward inter-domain communication and dynamic stability. Collectively, these findings indicate that the vaccine construct maintains structural flexibility crucial for its immunological role. **Figure 8A** shows the comparison of theoretical and experimental B-factors; **Figure 8B** illustrates residue-specific deformability; **Figure 8C** presents the eigenvalue distribution; **Figure 8D** depicts the atomic correlation map; and **Figure 8E** displays residue-residue correlations.

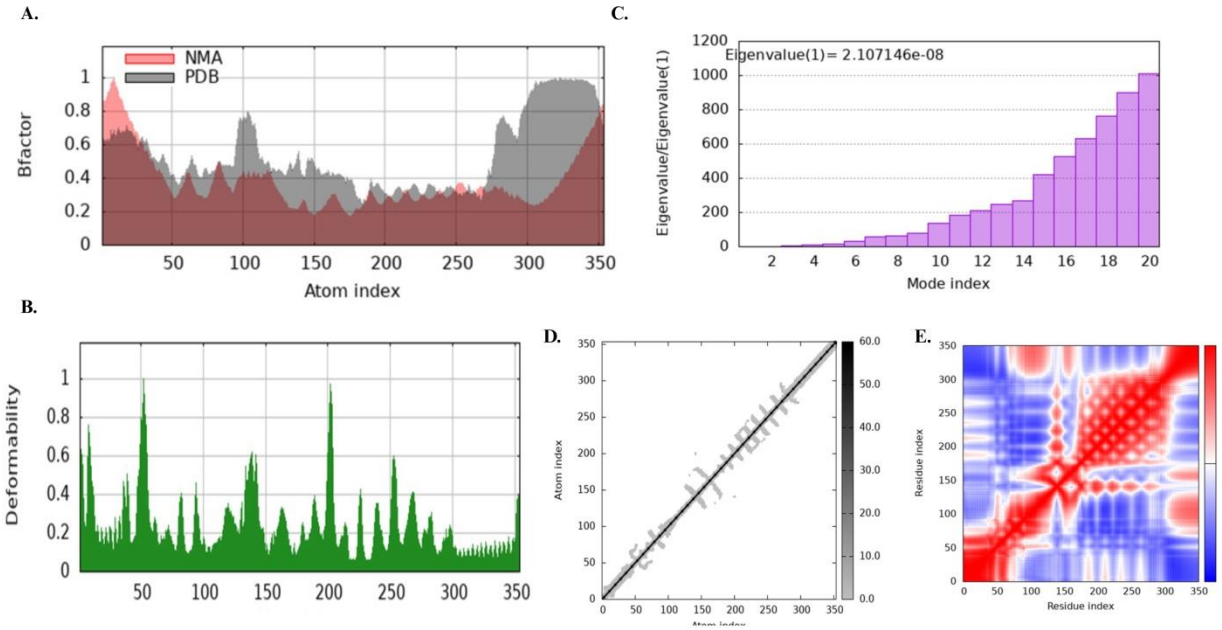

Figure 8. Normal Mode Analysis of Protein Dynamics. A) Comparison of theoretical and experimental B-factors; B) Residue-specific deformability; C) Eigenvalue distribution; D) Atomic correlation map; and E) Residue-residue correlations.

3.14 Codon Optimization and In Silico Cloning

To enhance expression efficiency in *Escherichia coli* K12, the vaccine gene sequence was codon-optimized using the JCat tool. The adapted sequence achieved a Codon Adaptation Index (CAI) of 1.0, indicating a high level of compatibility with the codon usage of the bacterial host. The GC content was adjusted to 53.03%, which closely aligns with the host's genomic GC content (˜50.73%), suggesting stable transcriptional and translational outcomes. The optimized gene preserved the correct reading frame, with no internal stop codons or frameshift mutations. Following optimization, the gene was inserted in silico into the RepX_pET28a(+) plasmid vector using Benchling software, enabling preparation for recombinant expression studies.

3.15 3D mRNA Structure Prediction and Docking with the 16S Ribosomal Subunit

The codon-optimized DNA sequence was transcribed into mRNA by incorporating essential regulatory elements, including the 5′ and 3′ untranslated regions (UTRs), a Kozak sequence, a signal peptide, a stop codon, and a poly(A) tail. To predict the secondary structure and evaluate thermodynamic stability, the RNAfold web server was utilized. The minimum free energy (MFE) structure exhibited a highly stable conformation with a free energy of −344.30 kcal/mol, while the ensemble free energy was calculated at −362.47 kcal/mol, indicating a robust overall stability across alternative structural forms. Notably, the MFE structure had a 0.00% ensemble frequency, highlighting the presence of multiple energetically favorable conformations that may facilitate efficient translation. To further assess

translational potential, the three-dimensional structure of the vaccine mRNA was modeled using the 3dRNA web server and docked with the *E. coli* 30S ribosomal subunit (PDB ID: 7OE1) via the HDOCK server. The resulting complex showed a high binding affinity (−421.36 kcal/mol), supporting strong interaction between the mRNA and ribosomal machinery. The centroid secondary structure, depicted in **Figure 8A**, represents the most thermodynamically stable folding pattern, marked by prominent stem-loop regions that contribute to its integrity. **Figure 8B** illustrates the base-pair probability plot, identifying regions with high pairing likelihoods and underscoring the stability of the predicted structure. The 3D structure of the mRNA, generated by the 3dRNA server and shown in **Figure 8C**, demonstrates the spatial organization necessary for efficient function. **Figure 8D** displays the docked complex of the mRNA with the 30S ribosomal subunit, revealing a well-fitted interaction interface that supports the construct's suitability for translation initiation within the host system.

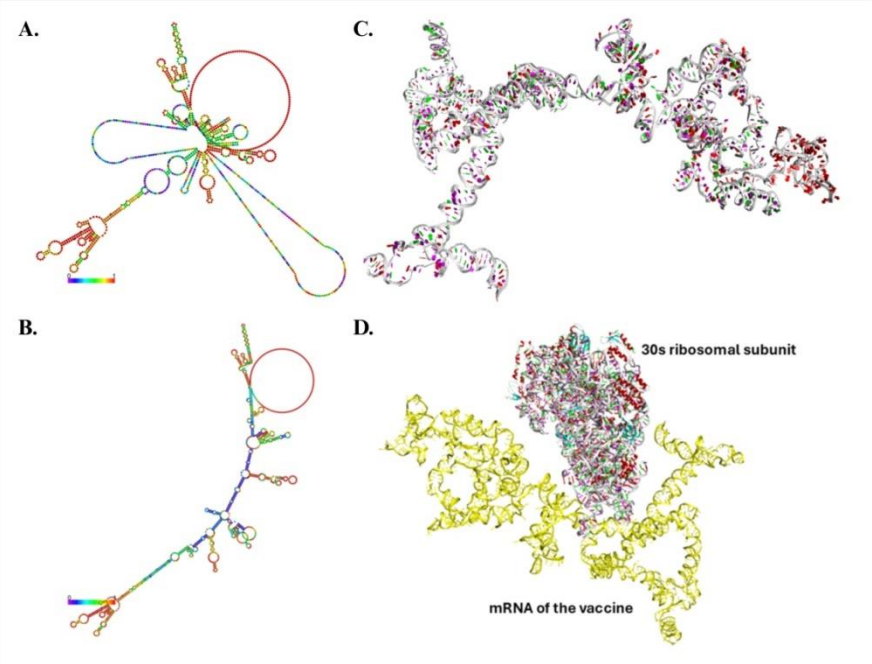

Figure 8. Structural image of the vaccine construct mRNA and its interaction with the *E. coli* ribosome. A) Centroid secondary structure of the mRNA, B) Base-pair probability distribution, C) 3D structure D) Docked mRNA-ribosome complex.

3. DISCUSSION

Pseudomonas aeruginosa is recognized as a formidable nosocomial pathogen due to its inherent resistance to multiple antibiotics and its remarkable environmental adaptability. Its categorization within the ESKAPE group and designation as a high-priority pathogen by the World Health Organization reflect the global demand for innovative therapeutic and prophylactic strategies. The increasing incidence of multidrug-resistant (MDR) strains has rendered many conventional antibiotics increasingly ineffective, thereby necessitating the exploration of alternative approaches, such as peptide-based vaccines. In this study, an immunoinformatics-driven strategy was employed to design a multi-epitope peptide vaccine targeting Flagellin A, a well-conserved, surface-exposed protein that is crucial for bacterial motility and host interaction. Flagellin A was chosen due to its significant role in both virulence and immune system activation. As a primary structural component of the bacterial flagellum, it is highly accessible to the host immune system. Moreover, its ability to interact directly with Toll-like receptor 5 (TLR5) makes it an efficient trigger of innate immune signaling. The conservation of both type A and type B variants of Flagellin A across *P. aeruginosa* strains further

enhances its value as a broad-spectrum vaccine candidate. The immunogenic characteristics of Flagellin A, particularly its ability to activate antigen-presenting cells (APCs) and stimulate T-cell responses, highlight its potential in epitope-based vaccine development. By targeting immunodominant regions capable of eliciting strong humoral and cellular immune responses, the designed multi-epitope construct shows promise as an effective candidate against drug-resistant *P. aeruginosa*. Overall, these findings support further research and experimental validation of this construct as a potential component of next-generation antimicrobial vaccine strategies.

This study employed an immunoinformatics-based approach to design a multi-epitope peptide vaccine targeting the Flagellin A protein of *Pseudomonas aeruginosa*. A comprehensive computational workflow was utilized to identify B-cell, CTL, and HTL epitopes with high antigenicity, while ensuring non-allergenicity and minimal similarity to human proteins to reduce adverse effects. The selected epitopes were validated for immunogenic potential using VaxiJen v2.0/v3.0 and AllerTOP v2.0, with BLASTp screening excluding cross-reactive sequences. Linkers and adjuvants were well incorporated to enhance immune stimulation and maintain construct stability. Molecular docking confirmed strong interactions between the vaccine and immune receptors, including MHC class I/II molecules and Toll-like receptors (TLR4 and TLR5), indicating the potential to activate both cellular and humoral immunity. Tertiary structure prediction via AlphaFold v3 and validation through Ramachandran plot supported structural reliability, while physicochemical analysis demonstrated favorable solubility, stability, and expression characteristics. Moreover, Codon optimization and in silico cloning into an *E. coli* expression system revealed high translational efficiency, confirmed by ribosomal docking and favorable mRNA secondary structure predictions. HLA-based population coverage analysis highlighted the vaccine potential to offer global protection, particularly for vulnerable and immunocompromised individuals. Overall, this integrative strategy underscores the value of reverse vaccinology in accelerating vaccine development against drug-resistant pathogens.

The selection of Flagellin A as a vaccine target was supported by its essential role in *P. aeruginosa* motility and structural integrity, as well as its conserved, surface-exposed nature. The retrieved sequence (P21184) exhibited strong immunogenic potential, indicated by a high VaxiJen antigenicity score and the absence of homology with human proteins, thereby minimizing the risk of cross-reactivity and autoimmune responses. Epitope prediction identified a significant number of immunodominant regions. BepiPred analysis revealed 25 linear B-cell epitopes, most of which were surface-accessible and favorable for antibody binding. Additionally, CTL and HTL epitope prediction based on strict binding affinity criteria (IC50 ≤ 100 nM) yielded 58 MHC class I and 68 MHC class II candidates. These epitopes provide a strong foundation for constructing a multi-epitope vaccine capable of eliciting both humoral and cellular immune responses. These findings highlight the strong immunological relevance of Flagellin A and support the design of epitope components for a peptide-based vaccine construct.

Incorporating antigenicity, non-allergenicity, and host non-homology criteria in epitope screening ensures a safe and targeted immune response against *P. aeruginosa*, mostly for combating multidrug-resistant strains.

The identification of B-cell and T-cell epitopes revealed several promising candidates for vaccine development. Antigenicity analysis by VaxiJen v2.0 showed that numerous predicted epitopes possess high immunogenic potential, with nine B-cell, 30 CTL, and 25 HTL epitopes exceeding the antigenicity threshold value. Subsequent allergenicity assessment using AllerTOP v2.1, identifying six B-cell, 14 CTL, and 10 HTL epitopes as both antigenic and non-allergenic, was making them suitable for inclusion in a multi-epitope vaccine. The lack of significant similarity to human proteins further enhances their safety by reducing the risk of autoimmune reactions. In addition, these results demonstrate the value of computational immunoinformatics in guiding the rational design of a safe and effective subunit vaccine against *P. aeruginosa*.

Molecular docking studies provided validation of T-cell epitope binding to MHC molecules, an important step in adaptive immune activation. The CTL epitope

ASLNTSLQR exhibited the strongest binding affinity with HLA-A11:01 (−189.76 kcal/mol), while the HTL epitope SKAGKDGSGAITSAV showed the highest affinity for DQB1*03:01:01:01. These strong interactions suggest their effective presentation by host immune cells, thereby supporting their inclusion in the final vaccine construct. Eight multi-epitope vaccine constructs were initially designed to explore the effects of epitope order and adjuvant inclusion on stability and immunogenic potential. Construct 7 emerged as the most promising based on its optimal physicochemical properties, high structural quality score 98.27, and strong antigenicity (1.0249 score).

The construct incorporated flexible linkers (AAY, GPGPG, and KK) and the D0 domain of Flagellin A as an adjuvant to enhance immunogenicity and structural integrity. Advanced structural modeling using AlphaFold v3 predicted a well-folded tertiary structure, which was further validated using Ramachandran plot and ERRAT analysis. The majority of residues fell within favored regions, with minor outliers involving glycine and proline, indicating acceptable flexibility without compromising overall stability. Dynamic behavior analysis via Normal Mode Analysis (NMA) highlighted favorable eigenvalues and B-factor distributions, suggesting structural stability and resilience under physiological conditions. The predicted flexibility in loop and terminal regions may aid in efficient antigen presentation. Additionally, C-ImmSim further affirmed the construct's immunogenic potential, showing a rapid IgM response followed by sustained IgG levels, memory cell generation, and strong T-helper and cytotoxic T-cell activity. Elevated levels of IFN-γ and IL-2 reinforced the vaccine's capacity to induce both humoral and cellular immunity.

Furthermore, Population coverage analysis demonstrated a global coverage of 62.54% with a PC90 value of 0.27, suggesting broad applicability across diverse HLA haplotypes for ensuring widespread vaccine effectiveness. Codon optimization for *E. coli* K12 resulted in a CAI value of 1.0 and a GC content of 53.03%, indicating compatibility with prokaryotic expression systems. In silico cloning into the pET28a(+) vector confirmed the feasibility of recombinant expression. Moreover, the predicted mRNA secondary structure showed favorable folding energetics, and docking with the 30S ribosomal subunit indicated high translational potential. However, Construct 7 demonstrates high structural stability, strong antigen presentation potential, broad population coverage, and suitability for expression in microbial systems. These findings suggest its viability as a next-generation vaccine candidate against drug-resistant *P. aeruginosa*. However, our results are highly promising, experimental validation through wet-lab studies remains essential to confirm its immunogenicity, safety, and protective efficacy.

CONCLUSION

We employed a rigorous immunoinformatics pipeline to design a multi-epitope peptide vaccine against *Pseudomonas aeruginosa*, focusing on the highly conserved, surface-exposed Flagellin A protein. By integrating rigorous criteria for antigenicity, non-allergenicity, and absence of human homology, we identified a panel of B-cell, CTL, and HTL epitopes capable of eliciting robust humoral and cellular responses. Among 8 vaccine constructs, "Construct 7" emerged as the lead candidate, demonstrating superior structural integrity (ERRAT 98.27; Ramachandran > 90% favored), strong predicted binding to MHC I/II and TLR4/TLR5 receptors, and favorable physicochemical properties for expression and solubility. Immune simulations forecasted rapid IgM and sustained IgG responses, potent T-cell activation, and memory formation. Codon optimization and in silico cloning confirmed high translational efficiency in *E. coli* K12, while population coverage analysis (62.54%) suggested broad applicability across diverse HLA haplotypes. This computationally designed vaccine requires experimental validation through in vitro expression and immunogenicity studies, followed by in vivo testing in appropriate animal models to assess safety, efficacy, and protective immunity. Further optimization of delivery methods and adjuvant formulations could enhance its clinical potential. Successful development of this vaccine may offer a vital tool in combating multidrug-resistant *P. aeruginosa* infections, reducing dependence on antibiotics, and addressing the urgent global challenge of antimicrobial resistance.

Abbreviations

Codon adaptation index (CAI), cytotoxic T lymphocyte (CTL), *Escherichia coli* (*E. coli*), error analysis tool (ERRAT), guanine-cytosine (GC) content, helper T lymphocyte (HTL), human leukocyte antigen (HLA), immunoglobulin G (IgG), immunoglobulin M (IgM), major histocompatibility complex (MHC), messenger ribonucleic acid (mRNA), *Pseudomonas aeruginosa* (*P. aeruginosa*), and Toll-like receptor (TLR).

Acknowledgments

The authors sincerely acknowledge the support and guidance received throughout the course of this research.

Author's Contributions

All authors contributed significantly to the design, execution, analysis, and interpretation of the study.

Funding

No external funding was received for this study.

Availability of Data

Data and materials used and/or analyzed during the current study are available from the corresponding author on reasonable request.

Ethics Approval and Consent to Participate

Not applicable.

Consent for Publication

Not applicable.

Competing Interests

The authors declare that they have no competing interests.

REFERENCES

1. Crone S, Vives-Flórez M, Kvich L, Saunders AM, Malone M, Nicolaisen MH, et al. The environmental occurrence of Pseudomonas aeruginosa. APMIS : acta pathologica, microbiologica, et immunologica Scandinavica. 2020;128(3):220-31.
2. Diggle SP, Whiteley M. Microbe Profile: Pseudomonas aeruginosa: opportunistic pathogen and lab rat. Microbiology (Reading, England). 2020;166(1):30-3.
3. Moradali MF, Ghods S, Rehm BHA. Pseudomonas aeruginosa Lifestyle: A Paradigm for Adaptation, Survival, and Persistence. Frontiers in Cellular and Infection Microbiology. 2017;Volume 7 - 2017.
4. Majeed MN, Iqbal A, Murtaza N, Herrera-Zúñiga LD, Siddique S, Raza M, et al. Designing a Multi-Epitope Vaccine Candidate to MERS-CoV: An in silico Approach. Innovative Biosystems and Bioengineering. 2024;8(3):3-17.
5. Hussein EF. Pseudomonas aeruginosa Represents a Main Cause of Hospital-Acquired Infections (HAI) and Multidrug Resistance (MDR). In: Darwesh O, Matter I, editors. Pseudomonas aeruginosa - New Perspectives and Applications. Rijeka: IntechOpen; 2022.
6. Wood SJ, Kuzel TM, Shafikhani SH. Pseudomonas aeruginosa: Infections, Animal Modeling, and Therapeutics. Cells. 2023;12(1):199.
7. Hilliam Y, Kaye S, Winstanley C. Pseudomonas aeruginosa and microbial keratitis. Journal of medical microbiology. 2020;69(1):3-13.
8. Kong KF, Schneper L, Mathee K. Beta-lactam antibiotics: from antibiosis to resistance and bacteriology. APMIS : acta pathologica, microbiologica, et immunologica Scandinavica. 2010;118(1):1-36.
9. Gaurav A, Bakht P, Saini M, Pandey S, Pathania R. Role of bacterial efflux pumps in antibiotic resistance, virulence, and strategies to discover novel efflux pump inhibitors. Microbiology (Reading, England). 2023;169(5).
10. Pang Z, Raudonis R, Glick BR, Lin T-J, Cheng Z. Antibiotic resistance in Pseudomonas aeruginosa: mechanisms and alternative therapeutic strategies. Biotechnology Advances. 2019;37(1):177-92.

11. Glen KA, Lamont IL. β-lactam Resistance in Pseudomonas aeruginosa: Current Status, Future Prospects. Pathogens (Basel, Switzerland). 2021;10(12).
12. Nathwani D, Raman G, Sulham K, Gavaghan M, Menon V. Clinical and economic consequences of hospital-acquired resistant and multidrug-resistant Pseudomonas aeruginosa infections: a systematic review and meta-analysis. Antimicrobial Resistance and Infection Control. 2014;3(1):32.
13. Tabak YP, Merchant S, Ye G, Vankeepuram L, Gupta V, Kurtz SG, et al. Incremental clinical and economic burden of suspected respiratory infections due to multi-drug-resistant Pseudomonas aeruginosa in the United States. The Journal of hospital infection. 2019;103(2):134-41.
14. Yang AF, Huang V, Samaroo-Campbell J, Augenbraun M. Multi-drug resistant Pseudomonas aeruginosa: a 2019-2020 single center retrospective case control study. Infection prevention in practice. 2023;5(3):100296.
15. Arora SK, Neely AN, Blair B, Lory S, Ramphal R. Role of motility and flagellin glycosylation in the pathogenesis of Pseudomonas aeruginosa burn wound infections. Infection and immunity. 2005;73(7):4395-8.
16. Song WS, Jeon YJ, Namgung B, Hong M, Yoon SI. A conserved TLR5 binding and activation hot spot on flagellin. Scientific reports. 2017;7:40878.
17. Campodónico VL, Llosa NJ, Grout M, Döring G, Maira-Litrán T, Pier GB. Evaluation of flagella and flagellin of Pseudomonas aeruginosa as vaccines. Infection and immunity. 2010;78(2):746-55.
18. Stanislavsky ES, Lam JS. Pseudomonas aeruginosa antigens as potential vaccines. FEMS Microbiology Reviews. 1997;21(3):243-77.
19. Oli AN, Obialor WO, Ifeanyichukwu MO, Odimegwu DC, Okoyeh JN, Emechebe GO, et al. Immunoinformatics and Vaccine Development: An Overview. ImmunoTargets and therapy. 2020;9:13-30
20. Negahdaripour M, Nezafat N, Eslami M, Ghoshoon MB, Shoolian E, Najafipour S, et al. Structural vaccinology considerations for in silico designing of a multi-epitope vaccine. Infection, Genetics and Evolution. 2018;58:96-109.

.